CCIT Report #484 May 2004

# Surface Wave Propagation Along a Metamaterial Cylindrical Guide

H. Cory and T. Blum
Department of Electrical Engineering
Technion—Israel Institute of Technology
Haifa 32000, Israel

**Abstract**

The dispersion relations for metamaterial cylindrical guides have been found and their Brillouin diagrams have been drawn for different parameters of the guides. It has been found that the transverse propagation coefficient of the first TMz mode and of the first TEz mode could be either real or imaginary. The longitudinal propagation coefficient of the first TMz mode starts at zero frequency and ends at a frequency where it is equal to the wave-number of the surrounding dielectric medium, while the longitudinal propagation coefficient of the first TEz mode starts at this same frequency and grows afterwards indefinitely. The first hybrid mode of order one as well as subsequent modes have also been studied. It has been found that for the first TMz and TEz modes, the group velocity is almost constant whether the transverse propagation coefficient is real or imaginary. Moreover, interesting coupling effects could be obtained by using adjacent metamaterial and dielectric cylindrical guides.

# 1. Introduction

Veselago [1] has shown that the Poynting vector of a plane wave is anti-parallel to its phase-velocity vector in materials whose permittivity and permeability are both negative. These materials have been consequently termed metamaterials, backward-wave materials, left-handed materials, and so on. Lindell et al. [2] and Lakhtakia et al. [3] have reviewed these materials. Pendry [4] has shown that a metamaterial slab can focus evanescent modes and resolve objects only a few nanometers wide in the optical domain. Ziolkowsky et al. [5] have studied metamaterials both analytically and numerically. Engheta [6] has made a theoretical analysis on thin subwavelength cavity resonators containing metamaterials. Alu et al. [7] have studied the radiation from a traveling current sheet at the interface between a conventional material and a metamaterial. Feise et al. [8] have investigated the effects of surface waves on the behavior of perfect lenses and studied metamaterial slabs with transition layers on either side. Cory et al. [9] have studied the longitudinal propagation coefficient dependence on frequency of regular modes having a real transverse wave-number. Wu et al. [10] have shown that additional modes having an imaginary transverse wave-number coexist with the regular modes. Cory et al. [11] have studied metamaterial slab coupling to another metamaterial slab or to a dielectric slab, taking into consideration regular trigonometric modes as well as hyperbolic modes. Baccarelli et al. [12] have investigated surface-wave propagation in a metamaterial grounded slab. Lakhtakia et al. [13] have shown that there exists a restricted equivalence between a thin bi-layer made of an epsilon-negative layer and a mu-negative layer and a thin single layer of a negative phase-velocity material. Finally, Qing et al. [14] have analyzed the Goos-Hänchen shift caused by total internal reflection at the interface between two media of the same or of opposite handedness.

The purpose of this letter is to analyze surface wave propagation along a metamaterial cylindrical guide. The TMz modes, the TEz modes, and the hybrid modes or order one have been studied, and the appropriate Brillouin diagrams have been drawn.

## 2. The dispersion equations

The potentials for a metamaterial cylindrical guide of radius $\rho = a$ are given as follows for an $\exp(j\omega t)$ time variation:

$$\psi_i^m = A_i B_{n,i}(k_{\rho i}\rho) \begin{Bmatrix} \cos n\varphi \\ \sin n\varphi \end{Bmatrix} \exp(-jk_z z) \qquad \text{(TMz modes)} \qquad (i = 1,2; n = 0,1,2,\dots) \tag{1a}$$

$$\psi_i^e = D_i B_{n,i}(k_{\rho i}\rho) \begin{Bmatrix} \sin n\varphi \\ \cos n\varphi \end{Bmatrix} \exp(-jk_z z) \qquad \text{(TEz modes)} \qquad (i = 1,2; n = 0,1,2,\dots)\,. \tag{1b}$$

$i = 1$ applies to the interior region ($\rho < a$) while $i = 2$ applies to the exterior region ($\rho > a$). $B_{n,i}(k_{\rho i}\rho)$ are appropriate Bessel functions of order $n$ ($n = 0,1,2,\dots$). We may chose $\cos n\varphi$ for the TMz mode and $\sin n\varphi$ for the TEz mode, or vice-versa. The tangential electric and magnetic field components of the *hybrid* modes can be retrieved as follows from these potentials:

$$E_{zi} = \frac{1}{j\omega\varepsilon_i}\left(\frac{\partial^2}{\partial z^2} + k_i^2\right)\psi_i^m \tag{2a}$$

$$E_{\varphi i} = \frac{1}{j\omega\varepsilon_i\rho}\frac{\partial^2\psi_i^m}{\partial\varphi\partial z} + \frac{\partial\psi_i^e}{\partial\rho} \tag{2b}$$

$$H_{zi} = \frac{1}{j\omega\mu_i}\left(\frac{\partial^2}{\partial z^2} + k_i^2\right)\psi_i^e \tag{3a}$$

$$H_{\varphi i} = \frac{1}{j\omega\mu_i\rho}\frac{\partial^2\psi_i^e}{\partial\varphi\partial z} - \frac{\partial\psi_i^m}{\partial\rho} \tag{3b}$$

where $i = 1,2$. $\varepsilon_1$ and $\mu_1$ are negative real numbers, $\varepsilon_2$ and $\mu_2$ are positive real numbers and

$$k_i^2 = \omega^2\varepsilon_i\mu_i = k_{\rho i}^2 + k_z^2 \quad (i = 1,2)\,. \tag{4}$$

The requirement that the tangential electric and magnetic field components be continuous at $\rho = a$ leads to a system of four homogeneous linear algebraic equations in $A_1, A_2, D_1, D_2$, which have a non-trivial solution only if the determinant of the coefficients of $A_1, A_2, D_1, D_2$, vanishes.

Thus, for the hybrid modes [15]

$$\begin{vmatrix} \varepsilon_2 k_{\rho 1}^2 B_{n,1}(k_{\rho 1}a) & 0 & |\varepsilon_1| k_{\rho 2}^2 B_{n,2}(k_{\rho 2}a) & 0 \\ 0 & \mu_2 k_{\rho 1}^2 B_{n,1}(k_{\rho 1}a) & 0 & |\mu_1| k_{\rho 2}^2 B_{n,2}(k_{\rho 2}a) \\ k_{\rho 1} B'_{n,1}(k_{\rho 1}a) & \frac{-k_z n}{\omega |\mu_1| a} B_{n,1}(k_{\rho 1}a) & -k_{\rho 2} B'_{n,2}(k_{\rho 2}a) & \frac{-k_z n}{\omega \mu_2 a} B_{n,2}(k_{\rho 2}a) \\ \frac{-k_z n}{\omega |\varepsilon_1| a} B_{n,1}(k_{\rho 1}a) & k_{\rho 1} B'_{n,1}(k_{\rho 1}a) & \frac{-k_z n}{\omega \varepsilon_2 a} B_{n,2}(k_{\rho 2}a) & -k_{\rho 2} B'_{n,2}(k_{\rho 2}a) \end{vmatrix} = 0 \qquad (5)$$

where the derivatives ($'$) have been taken with respect to the arguments of the appropriate Bessel functions (see below). Equation (5) can be solved numerically. It has been found that in the interior region ($i = 1$), in addition to the real solutions $k_{\rho i} \triangleq \alpha_1$ ($\alpha_1 > 0$) for which $B_{n,1}(k_{\rho 1}\rho) = J_n(\alpha_1 \rho)$, there are imaginary solutions $k_{\rho 1} \triangleq -j\alpha_1$ ($\alpha_1 > 0$) as well, for which $B_{n,1}(k_{\rho 1}\rho) = I_n(\alpha_1 \rho)$. In the exterior region ($i = 2$), $k_{\rho 2}$ is imaginary since the waves decay outside the guide, i.e. $k_{\rho 2} = -j\alpha_2$ ($\alpha_2 > 0$) so that $B_{n,2}(k_{\rho 2}\rho) = K_n(\alpha_2 \rho)$. It should be noted that $\frac{\partial}{\partial \rho} J_n(\alpha_1 \rho) \triangleq \alpha_1 J'_n(\alpha_1 \rho)$, $\frac{\partial}{\partial \rho} I_n(\alpha_1 \rho) \triangleq \alpha_1 I'_n(\alpha_1 \rho)$, and $\frac{\partial}{\partial \rho} K_n(\alpha_2 \rho) \triangleq \alpha_2 K'_n(\alpha_2 \rho)$.

We obtain for the TMz modes ($n = 0, D_1 = D_2 = 0$) and for the TEz modes ($n = 0, A_1 = A_2 = 0$) the following relations deduced from eq. (5):

$$\varepsilon_2(\alpha_1 a) \begin{Bmatrix} J_0(\alpha_1 a) \\ I_0(\alpha_1 a) \end{Bmatrix} K'_0(\alpha_2 a) - |\varepsilon_1|(\alpha_2 a) \begin{Bmatrix} J'_0(\alpha_1 a) \\ I'_0(\alpha_1 a) \end{Bmatrix} K_0(\alpha_2 a) = 0 \qquad \text{(TMz modes)} \qquad (6a)$$

$$\mu_2(\alpha_1 a) \begin{Bmatrix} J_0(\alpha_1 a) \\ I_0(\alpha_1 a) \end{Bmatrix} K'_0(\alpha_2 a) - |\mu_1|(\alpha_2 a) \begin{Bmatrix} J'_0(\alpha_1 a) \\ I'_0(\alpha_1 a) \end{Bmatrix} K_0(\alpha_2 a) = 0 \qquad \text{(TEz modes)} \qquad (6b)$$

where $J_0(\alpha_1 a)$ and $J'_0(\alpha_1 a)$ apply when $k_{\rho 1}$ is real while $I_0(\alpha_1 a)$ and $I'_0(\alpha_1 a)$ apply when $k_{\rho 1}$ is imaginary. It should be noted that $J'_0(\alpha_1 a) = -J_1(\alpha_1 a)$, $I'_0(\alpha_1 a) = I_1(\alpha_1 a)$ and $K'_0(\alpha_2 a) = -K_1(\alpha_2 a)$.

We deduce from eq. (4) that

$$\pm(\alpha_1 a)^2 + (k_z a)^2 = \omega^2 |\varepsilon_1| |\mu_1| a^2 \qquad (7a)$$

where the + sign applies when $k_{\rho 1}$ is real and the − sign applies when $k_{\rho 1}$ is imaginary. Also since $k_{\rho 2}$ is always imaginary, it follows that $k_{\rho 2}^2$ is a negative real number so that

$$-(\alpha_2 a)^2 + (k_z a)^2 = \omega^2 \varepsilon_2 \mu_2 a^2 \,. \qquad (7b)$$

Therefore, if $k_{\rho 1}$ is real we obtain

$$(\alpha_2 a)^2 + (\alpha_1 a)^2 = \omega^2(|\varepsilon_1||\mu_1| - \varepsilon_2\mu_2)a^2 \tag{8a}$$

which is the equation of a circle, while if $k_{\rho 1}$ is imaginary, we obtain

$$(\alpha_2 a)^2 - (\alpha_1 a)^2 = \omega^2(|\varepsilon_1||\mu_1| - \varepsilon_2\mu_2)a^2 \tag{8b}$$

which is the equation of an hyperbola. The values of $\alpha_1$ and $\alpha_2$ could be found by solving numerically the pair of equations (8a) for real $k_{\rho 1}$ or (8b) for imaginary $k_{\rho_1}$ and (6b) for TEz modes or (6a) for TMz modes or (5) for hybrid modes. The value of $k_z$ could be found afterwards from equations (7a) or (7b). A similar pattern has been observed for surface wave propagation along metamaterial slabs [11].

We shall study more particularly the behavior of the first TMz and TEz modes with respect to frequency. Graphs giving $\alpha_2 a$ as a function of $\alpha_1 a$ (or vice-versa), with $\varepsilon_{r1} = -2$, $\mu_{r1} = -1$, $\varepsilon_{r2} = 1$, $\mu_{r2} = 1$, are given in Fig. (1a) for these modes. They describe eqs. (6a) and (6b). Let us denote by $a, b, c$ and $d$ the sections of these graphs corresponding to real $k_{\rho 1}$ for the TMz mode, imaginary $k_{\rho 1}$ for the TMz mode, real $k_{\rho 1}$ for the TEz mode, and imaginary $k_{\rho 1}$ for the TEz mode, respectively. For zero frequency, the hyperbola given by eq. (8b) degenerates into a straight line for which $\alpha_1 = \alpha_2$. The value of $\alpha_1$ (or $\alpha_2$) is given by solving eq. (6a) with $I_0(\alpha_1 a)$ and $I_0'(\alpha_1 a)$ for $\alpha_1 = \alpha_2$. This straight line cuts section $b$ at point (1) and does not cut section $d$. When the frequency grows, successive hyperbolas given by eq. (8b) cut section $b$ up to point (2) where $\alpha_1 = 0$. The corresponding value of $\alpha_2$ is found by substituting $\alpha_1 = 0$ into eq. (6a). The adequate transcendental equation to solve is given as follows:

$$\frac{K_1(\alpha_2 a)}{(\alpha_2 a)K_0(\alpha_2 a)} = \frac{|\varepsilon_1|}{2\varepsilon_2} \qquad \text{(TMz mode)}\,. \tag{9a}$$

If $|\varepsilon_1| = \varepsilon_2$, the solution to this equation does not depend on $|\mu_1|$ or $\mu_2$. When frequency grows further, successive circles given by eq. (8a) cut section $a$ up to point (3) (which is common to both modes), where $\alpha_2 = 0$. The corresponding value of $\alpha_1$ is found by substituting $\alpha_2 = 0$ into eqs. (6a) or (6b). The adequate equations to solve are given by

$$\frac{\varepsilon_2(\alpha_1 a)J_0(\alpha_1 a)}{|\varepsilon_1|J_1(\alpha_1 a)} = 0 \qquad \text{(TMz mode)} \tag{9b}$$

$$\frac{\mu_2(\alpha_1 a)J_0(\alpha_1 a)}{|\mu_1|J_1(\alpha_1 a)} = 0 \qquad \text{(TEz mode)} \tag{9c}$$

i.e., for both modes, by $\alpha_1 a = 2.405$, which is the first zero of Bessel's function of order zero. When frequency grows further, successive circles given by eq. (8a) cut section $c$ up to point (4) where $\alpha_1 = 0$. The corresponding value of $\alpha_2$ is found by substituting $\alpha_1 = 0$ into eq. (6b). The adequate transcendental equation to solve is given as follows:

$$\frac{K_1(\alpha_2 a)}{(\alpha_2 a)K_0(\alpha_2 a)} = \frac{|\mu_1|}{2\mu_2} \qquad \text{(TEz mode)}\,. \tag{9d}$$

If $|\mu_1| = \mu_2$, the solution to this equation does not depend on $|\varepsilon_1|$ or $\varepsilon_2$. When frequency grows further, successive hyperbolas given by eq. (8b) cut then section $d$, giving points such as (5).

The graph of $k_z a$ as a function of $k_2 a$ with the same values of permittivity and permeability as in Fig. (1a), is given in Fig. (1b) for the first TMz and TEz modes. The points (1) to (5) in Fig. (1b) correspond to the same points in Fig. (1a). It is interesting that for both modes, the group velocity $v_g = \frac{\partial \omega}{\partial k_z}$ is almost constant, whether $k_{\rho 1}$ is real or imaginary. The first TMz mode starts at $\omega = 0$ where $\alpha_1 = \alpha_2$ and ends at $\omega = \alpha_1/\sqrt{|\varepsilon_1||\mu_1| - \varepsilon_2\mu_2}$ where $\alpha_1 = 2.405$ and $\alpha_2 = 0$. It should be noted that at this point, $k_z = k_2$. The first TEz mode starts at the same $\omega$ where the first TMz mode ends and tends afterwards to infinity. If we now chose $\varepsilon_{r1} = -1$, $\mu_{r1} = -2$ instead of $\varepsilon_{r1} = -2$, $\mu_{r1} = -1$, keeping $\varepsilon_{r2} = 1$, $\mu_{r2} = 1$, the curves for the TMz modes and for the TEz modes interchange.

## 3. Numerical results

The variation of $\alpha_2 a$ versus $\alpha_1 a$ and of $k_z a$ versus $k_z a$ for the following two sets of data: a) $\varepsilon_{r1} = -2$, $\mu_{r1} = -1$, $\varepsilon_{r2} = 1$, $\mu_{r2} = 1$, b) $\varepsilon_{r1} = -5$, $\mu_{r1} = -1$, $\varepsilon_{r2} = 1$, $\mu_{r2} = 1$, is given in Figs. 2(a), 2(b), 3(a) and 3(b), respectively, for successive TMz and TEz modes and for successive hybrid modes of order one. It can be seen in Figs. (2a) and (3a) that for the first TEz mode, the value of $\alpha_2 a$ corresponding to $\alpha_1 = 0$ is given by eq. (9d), i.e. $\alpha_2 a = 2.387$ (point (4)), whether $|\varepsilon_1| = -2$ or $-5$, since $|\mu_1| = \mu_2$, as predicted in the previous section. Moreover, for the first TMz mode, the value of $\alpha_2 a$ corresponding to $\alpha_1 = 0$ is given by eq. (9a), i.e. $\alpha_2 a = 1.332$ (point (2)) for $|\varepsilon_1| = -2$ and 0.651 (point (2)) for $|\varepsilon_1| = -5$. It can further be seen in Figs. (2a) and (3a) that for $\alpha_2 = 0$, we obtain $\alpha_1 a = 2.405$ (point (3)), i.e. the first zero of Bessel's function of order zero, for the first

TMz and TEz modes, as predicted in the previous section, while we obtain $\alpha_1 a = 5.520, 8.654, \ldots$, i.e. the successive (second, third, ... ) zeroes of Bessel's function of order zero, for the successive (second, third, ... ) TMz and TEz modes, because these $\alpha_1 a$'s are the solutions of eqs. (9b) and (9c). The values of $\alpha_1 a$ for $\alpha_2 = 0$ depend on the geometry of the device but not on its composition. Reverting to the hybrid modes of order one, we can see in Figs. (2a) and (3a) that for $\alpha_2 = 0$, we obtain $\alpha_1 a = 3.832, 7.016, \ldots$, which are the successive (first, second, ... ) zeroes of Bessel's function of order one, because these $\alpha_1 a$'s are the solutions of eq. (5) for $\alpha_2 = 0$ and $n = 1$. It can also be seen in Figs. (2a) and (3a) that the value of $\alpha_2 a$ for $\alpha_1 = 0$ is obtained for the hybrid modes of order one by solving eq. (5) for $\alpha_2 a$ with $\alpha_1 = 0$ and $n = 1$. It is interesting to note that the first hybrid mode of order one, as well as the first TMz and TEz modes, have imaginary solutions for $k_{\rho 1}$. The next (second, third, ... ) TMz and TEz modes tend asymptotically to infinity for $\alpha_1 a = 3.832, 7.016, \ldots$, while the next (second, third, ... ) hybrid modes of order one tend asymptotically to infinity for $\alpha_1 a = 2.405, 5.520, \ldots$ . This behaviour can be explained as follows: We obtain from eqs. (6a) and (6b) that:

$$\alpha_1 a = \alpha_2 a \frac{|\varepsilon_1| J_1(\alpha_1 a) K_0(\alpha_2 a)}{\varepsilon_2 J_0(\alpha_1 a) K_1(\alpha_2 a)} \qquad \text{(TMz modes)} \tag{10a}$$

$$\alpha_1 a = \alpha_2 a \frac{|\mu_1| J_1(\alpha_1 a) K_0(\alpha_2 a)}{\mu_2 J_0(\alpha_1 a) K_1(\alpha_2 a)} \qquad \text{(TMz modes)}\,. \tag{10b}$$

For large $\alpha_2 a, K_0(\alpha_2 a) \sim K_1(\alpha_2 a)$ and they are both positive. Moreover $\alpha_1 a$ and $\alpha_2 a$ are always positive. Therefore, for the TMz and the TEz modes, only when $J_0(\alpha_1 a)$ and $J_1(\alpha_1 a)$ have the same sign, is there a solution to eqs. (10a) and (10b). This is the reason for the appearance of the stopbands in the TMz and the TEz modes, which occur between the i'th zero of $J_0$ and that of $J_1, (i = 1, 2, 3, \ldots)$. The stopbands in the hybrid modes of order one can be deduced similarly.

It can be seen in Figs. 2(b) and 3(b) that the TMz and TEz modes other than the first (i.e. the second, the third, ... ), start together on the $k_z = k_2$ curve where $\omega = \alpha_1 / \sqrt{|\varepsilon_1||\mu_1| - \varepsilon_2 \mu_2}$, $\alpha_1 a = 5.520, 8.654, \ldots$ , $\alpha_2 = 0$, and tend asymptotically towards the $k_z = k_1$ curve.

## 4. Conclusion

The Brillouin diagrams of metamaterial cylindrical guides have been drawn for different parameters of the guides. It has been found that the transverse propagation coefficient of the first TMz mode,

of the first TEz mode and of the first hybrid mode of order one, could be either real or imaginary. The longitudinal propagation coefficient of the first TMz mode starts at zero frequency and ends at a frequency where it is equal to the wave-number of the surrounding dielectric medium, while the longitudinal propagation coefficient of the first TEz mode starts at this same frequency and tends afterwards to infinity. It is interesting to note that the first TMz mode is the dominant mode in a metamaterial cylindrical guide but that it possesses a lower cut-off frequency in a dielectric cylindrical guide, so that if it was possible to excite both in this mode, useful coupling effects could be obtained as in the corresponding case of coupled metamaterial and dielectric slabs [11].

**Acknowledgment.** One of the authors (Haim Cory) would like to thank the Fund for the Promotion of Research at the Technion for supporting this research.

## References


[1] V.G. Veselago, The electrodynamics of substances with simultaneously negative values of $\varepsilon$ and $\mu$, Soviet Phys Uspekhi 10 (1968), 509–514.

[2] I.V. Lindell, S.A. Tretyakov, K.I. Nikoskinen, and S. Ilvonen, BW media: Media with negative parameters, capable of supporting backward waves, Microwave Opt Technol Lett 31 (2001), 129–133.

[3] A. Lakhtakia, M.W. McCall, and W.S. Weiglhofer, Brief overview of recent developments on negative phase-velocity mediums (alias left-handed materials), Int J Electron Commun (AEÜ) 56 (2002), 407–410.

[4] J.B. Pendry, Negative refraction makes a perfect lens, Phys Rev Lett 85 (2000), 3966–3969.

[5] R.W. Ziolkowsky, and E. Heyman, Wave propagation in media having negative permittivity and permeability, Physical Rev E 64 (2001), 056625.

[6] N. Engheta, An idea for thin sub-wavelength cavity resonators using metamaterials with negative permittivity and permeability, IEEE Antenna and Wireless Propagat Lett 1 (2002), 10–13.

[7] A. Alu, and N. Engheta, Radiation from a traveling-wave current sheet at the interface between a conventional material and a metamaterial with negative permittivity and permeability, Microwave Opt Technol Lett 35 (2002), 460–463.

[8] M.W. Feise, P.J. Bevelacqua, and J.B. Schneider, Effect of surface waves on the behavior of perfect lenses, Physical Rev B 66 (2002), 035113.

[9] H. Cory, and A. Barger, Surface wave propagation along a metamaterial slab, Microwave Opt Technol Lett 38 (2003), 392–395.

[10] B.-I. Wu, T.M. Grzegorczyk, Y. Zhang, and J.A. Kong, Guided modes with imaginary transverse wavenumber in a slab waveguide with negative permittivity and permeability, J Appl Phys 93 (2003), 9386–9388.

[11] H. Cory, and O. Skorka, Metamaterial slabs coupling, Microwave Opt Technol Lett 40 (2004), 340–344.

[12] P. Baccarelli, B. Burghignoli, G. Lovat and S. Paulotto, Surface-wave suppression in a double-negative metamaterial grounded slab, IEEE Antennas Wireless Propagat Lett 2 (2003), 269–272.

[13] A. Lakhtakia and C. M. Krowne, Restricted equivalence of paired epsilon-negative and mu-negative layers to a negative phase-velocity material (alias left-handed material) Optik 114 (2003), 305–307.

[14] D.-K. Qing and G. Chen, Goos Hänchen shifts at the interfaces between left-and right-handed media, Optics Lett 29 (2004), 872–874.

[15] R. Harrington, Time-harmonic electromagnetic fields, Mc-Graw Hill (1961).

## Figure Captions

Figure 1: (a) $\alpha_2 a$ versus $\alpha_1 a$ for the first TMz and TEz modes.

$\varepsilon_{r1} = -2$, $\mu_{r1} = -1$; $\varepsilon_{r2} = 1$, $\mu_{r2} = 1$.

| | | | |
|---|---|---|---|
| $+\ +\ +$: | TMz mode, real $k_{p1}$. | $\circ\ \circ\ \circ$: | TMz mode, imaginary $k_{p1}$. |
| $*\ *\ *$ : | TEz mode, real $k_{p1}$. | $\bullet\ \bullet\ \bullet$: | TEz mode, imaginary $k_{p1}$. |

(b) $k_z a$ versus $k_2 a$ for the first TMz and TEz modes.

$\varepsilon_{r1} = -2$, $\mu_{r1} = -1$; $\varepsilon_{r2} = 1$, $\mu_{r2} = 1$.

| | | | |
|---|---|---|---|
| $+\ +\ +$: | TMz mode, real $k_{p1}$. | $\circ\ \circ\ \circ$: | TMz mode, imaginary $k_{p1}$. |
| $*\ *\ *$ : | TEz mode, real $k_{p1}$. | $\bullet\ \bullet\ \bullet$: | TEz mode, imaginary $k_{p1}$. |

Figure 2: (a) $\alpha_2 a$ versus $\alpha_1 a$ for the TMz modes, the TEz modes, and the hybrid modes of order one;

$\varepsilon_{r1} = -2$, $\mu_{r1} = -1$; $\varepsilon_{r2} = 1$, $\mu_{r2} = 1$.

| | | | |
|---|---|---|---|
| $+\ +\ +$: | TMz mode, real $k_{p1}$. | $\circ\ \circ\ \circ$: | TMz mode, imaginary $k_{p1}$. |
| $*\ *\ *$ : | TEz mode, real $k_{p1}$. | $\bullet\ \bullet\ \bullet$: | TEz mode, imaginary $k_{p1}$. |
| $\times\ \times\ \times$: | hybrid mode, real $k_{p1}$. | $\square\square\square$: | hybrid mode, imaginary $k_{p1}$. |

(b) $k_z a$ versus $k_2 a$ for the TMz modes, the TEz modes, and the hybrid modes of order one.

$\varepsilon_{r1} = -2$, $\mu_{r1} = -1$; $\varepsilon_{r2} = 1$, $\mu_{r2} = 1$.

| | | | |
|---|---|---|---|
| $+\ +\ +$: | TMz mode, real $k_{p1}$. | $\circ\ \circ\ \circ$: | TMz mode, imaginary $k_{p1}$. |
| $*\ *\ *$ : | TEz mode, real $k_{p1}$. | $\bullet\ \bullet\ \bullet$: | TEz mode, imaginary $k_{p1}$. |
| $\times\ \times\ \times$: | hybrid mode, real $k_{p1}$. | $\square\square\square$: | hybrid mode, imaginary $k_{p1}$. |

Figure 3: (a) $\alpha_2 a$ versus $\alpha_1 a$ for the TMz modes, the TEz modes, and the hybrid modes of order one.

$\varepsilon_{r1} = -5$, $\mu_{r1} = -1$; $\varepsilon_{r2} = 1$, $\mu_{r2} = 1$.

| | | | |
|---|---|---|---|
| $+\ +\ +$: | TMz mode, real $k_{p1}$. | $\circ\ \circ\ \circ$: | TMz mode, imaginary $k_{p1}$. |
| $*\ *\ *$ : | TEz mode, real $k_{p1}$. | $\bullet\ \bullet\ \bullet$: | TEz mode, imaginary $k_{p1}$. |
| $\times\ \times\ \times$: | hybrid mode, real $k_{p1}$. | $\square\square\square$: | hybrid mode, imaginary $k_{p1}$. |

(b) $k_z a$ versus $k_2 a$ for the TMz modes, the TEz modes, and the hybrid modes of order one.

$\varepsilon_{r1} = -5$, $\mu_{r1} = -1$; $\varepsilon_{r2} = 1$, $\mu_{r2} = 1$.

| | | | |
|---|---|---|---|
| $+\ +\ +$: | TMz mode, real $k_{p1}$. | $\circ\ \circ\ \circ$: | TMz mode, imaginary $k_{p1}$. |
| $*\ *\ *$ : | TEz mode, real $k_{p1}$. | $\bullet\ \bullet\ \bullet$: | TEz mode, imaginary $k_{p1}$. |
| $\times\ \times\ \times$: | hybrid mode, real $k_{p1}$. | $\square\square\square$: | hybrid mode, imaginary $k_{p1}$. |

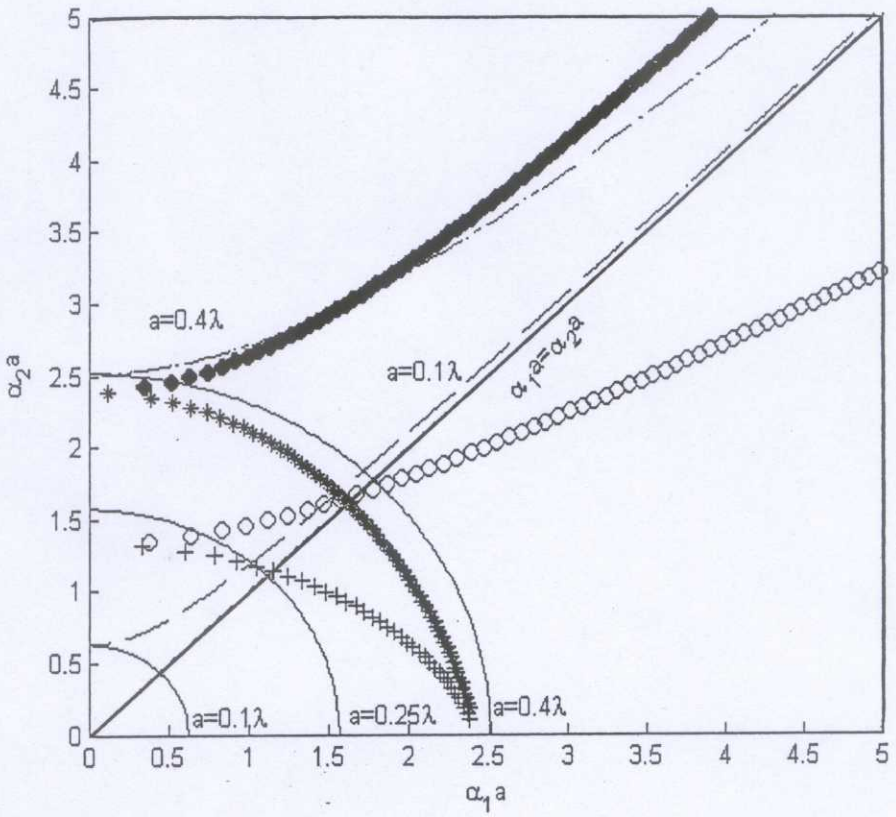


Figure 1 (a)

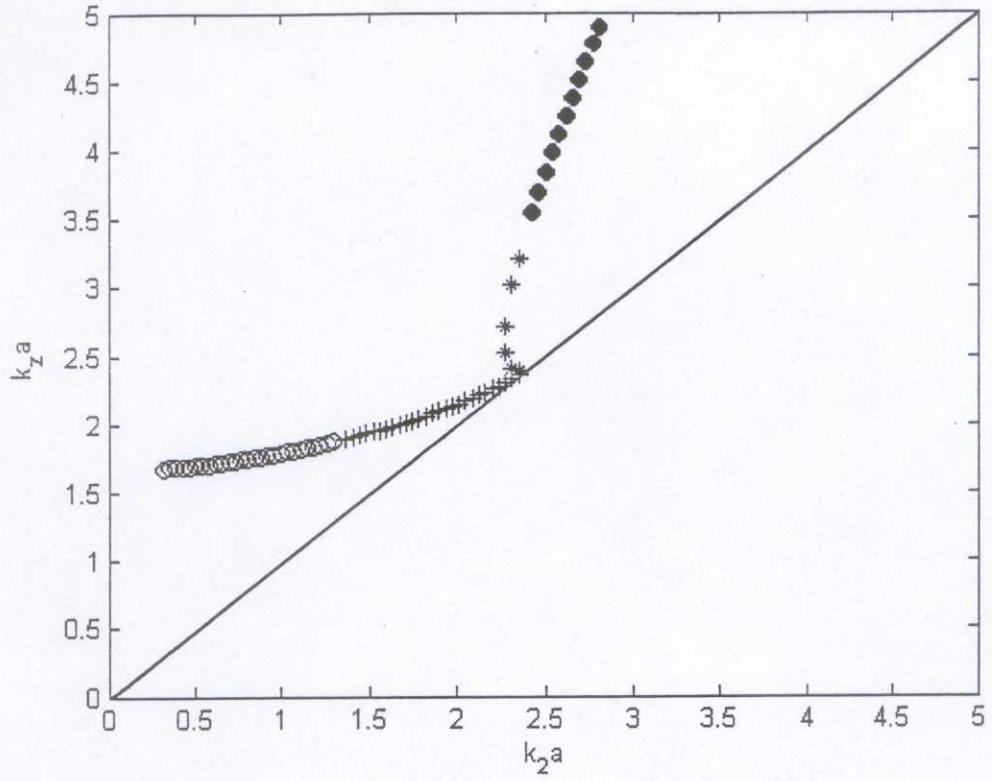


Figure 1 (b)

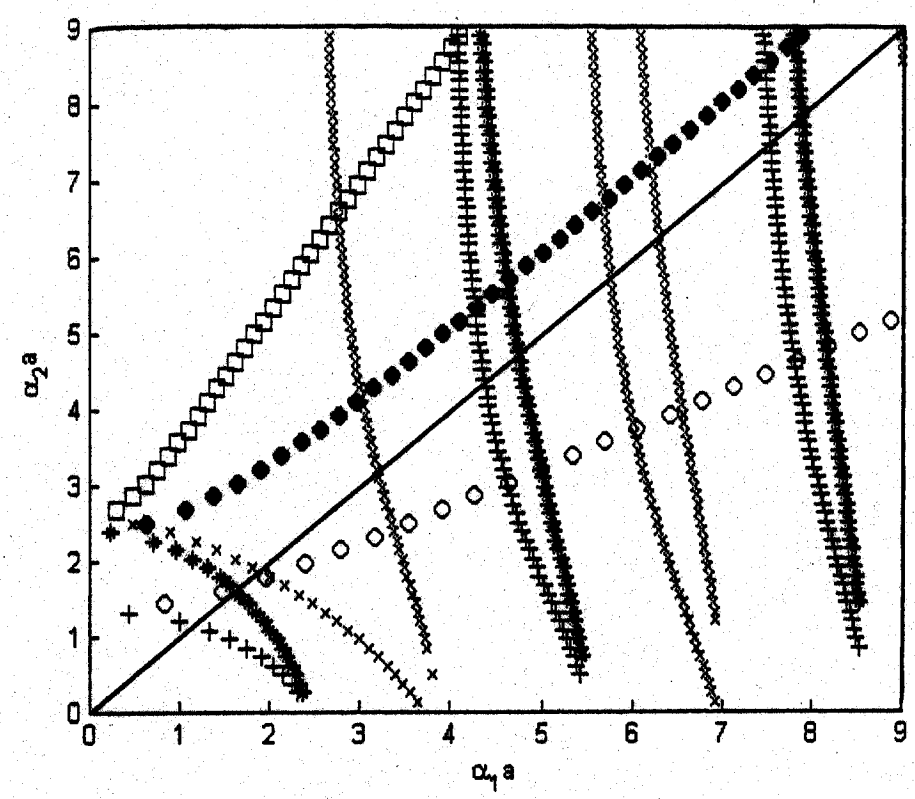


Figure 2: (a)

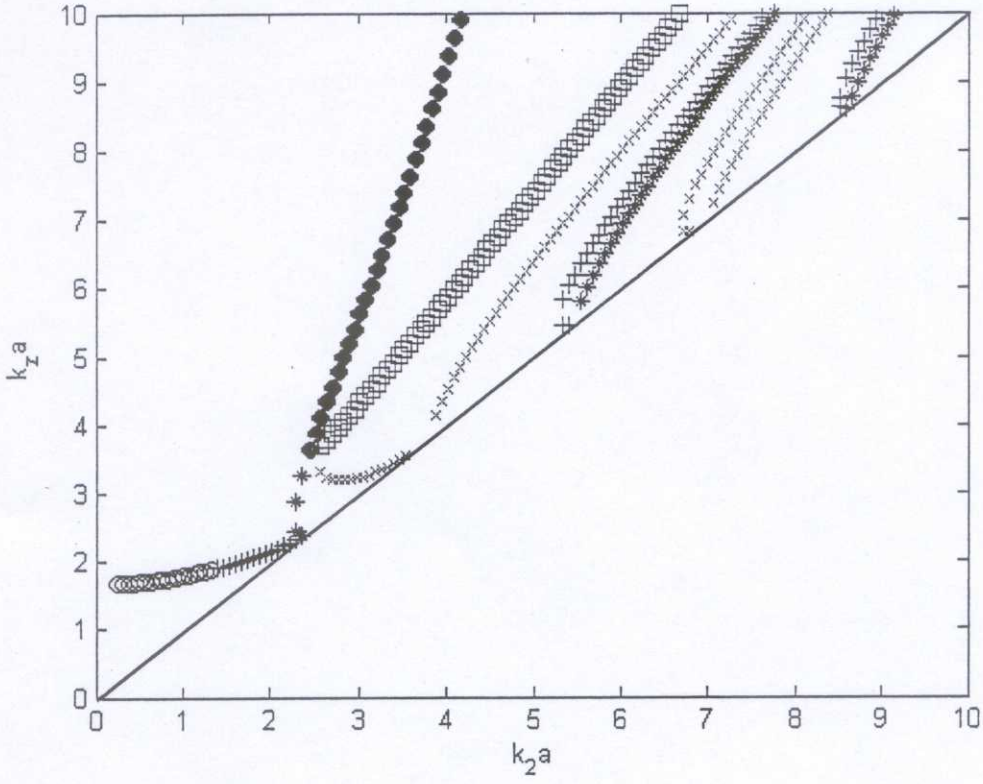


Figure 2 (b)

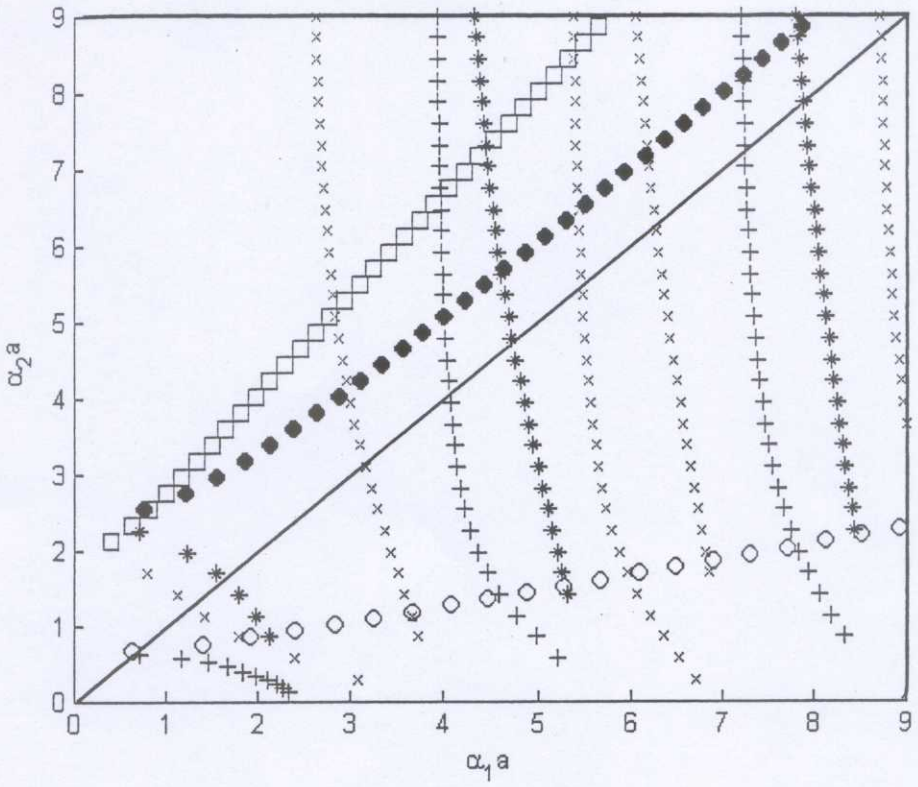


Figure 3 (a)

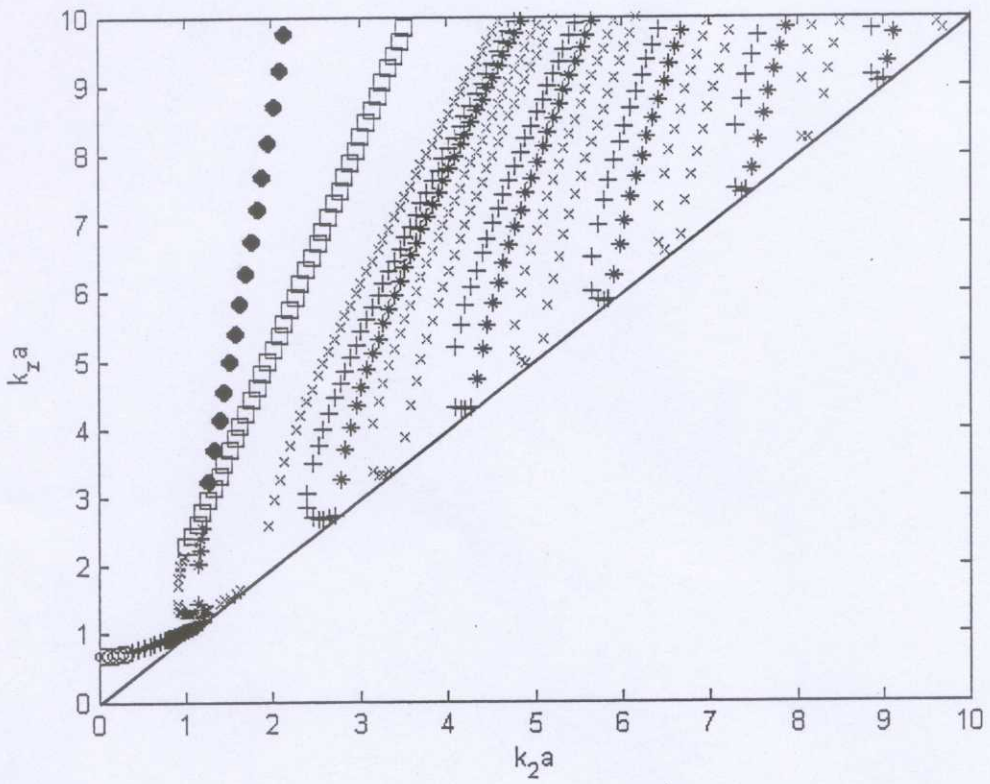


Figure 3 (b)